Application and validation of a viscosity approach to the existence of nanogratings in oxide glasses

# A viscosity approach to the existence of nanogratings in oxide glasses

Qiong Xie[1], Maxime Cavillon[1,*], Bertrand Poumellec[1], Diego Pugliese[2], Davide Janner[2], and Matthieu Lancry[1]

[1]Institut de Chimie Moléculaire et des Matériaux d'Orsay (ICMMO), Université Paris-Saclay, CNRS, 91405 Orsay, France
[2]Department of Applied Science and Technology (DISAT) and RU INSTM, Politecnico di Torino, 10129 Torino, Italy
*Corresponding author: maxime.cavillon@universite-paris-saclay.fr

**Abstract**

Nanogratings are self-organized and sub-wavelength birefringent structures that are formed upon the action of high intensity ultrashort light pulses in the bulk of a transparent material. They have found interest in optics/photonics, microfluidics, optical data storage or again sensing applications. However, the ability to successfully imprint 3-dimensional (3D) nanogratings in silicate glasses is a strong function of the glass composition. In this work, we investigate the role of glass viscosity on the ability to induce these nanogratings. We first investigate the nanogratings formation window in an energy-repetition rate laser parameter landscape for five common oxide glasses: $SiO_2$ (Suprasil), $GeO_2$, and Schott glasses AF32, Borofloat, and BK7. Secondly, and based on previous work, we define a domain of existence of the nanogratings using viscosity-based arguments. The lower limit corresponds to a temperature at which the viscosity is ~$10^{6.6}$ Pa·s, where occurs nanocavitation of the glass, forming the nanopores that compose the nanogratings. An upper temperature limit, set for a viscosity value of ~$10^{3.0}$ Pa·s, relates to either collapse or growth of the nanopores, resulting in the erasure of the nanopores, hence the nanogratings. The experimental results agree with the predictions made by this viscosity approach and literature data. This work opens the door to future glass viscosity engineering to maximize 3D nanogratings imprinting.

## I. Introduction

Nanogratings, also labeled as "Type II" transformations, were first observed in 2003 [1] after femtosecond (fs) laser irradiation inside silica glass. These nanostructures exhibit the remarkable property of being birefringent with a slow/fast axis that can be spatially controlled through light properties such as polarization. Original properties can arise from these nanostructures, such as anisotropic light scattering, linear dichroism, chiral optical properties, and high thermal stability [2], [3]. To harvest these properties and since their discovery, they have therefore driven strong interest for applications including 3D geometric phase optics and micro optical polarization sensitive elements, 5D optical data storage, microfluidics, or temperature/pressure fiber-based sensors etc. [4]–[9].

In the pioneering work of Ref. [1], the authors proposed that the existence of these sub-wavelength and pseudo-organized structures, yielding to birefringence, originated from the interference between the incident light field and the plasma induced by ultrashort laser pulses. Electronic inhomogeneities were proposed as the triggering cause of this coupling mechanism. In 2008 a transient nanoplasmonics model was introduced [10], describing the appearance of spherical nanoplasma preferentially located at the hot spots induced by localized multiphoton ionization at defects or color center locations. In this view, the nanoplasma would experience an asymmetric growth oriented preferentially in the direction perpendicular to the laser polarization, due to a local field enhancement. It would then move from a spherical to an ellipsoidal shape, and ultimately to disk-like shape, as more pulses are deposited inside the focal volume. Moreover, an exciton-polariton model was thus proposed in 2012 [11], through the coupling of light with plasmons. Later results suggested that these nanogratings originated from nanometric or sub-nanometric heterogeneities initially present in the glass, leading to coherently interfering scattering wavelets, hence the formation of a standing wave (2014: [12], and 2016: [13]). It is worth pointing out that this process is reinforced by a pulse-to-pulse effect, and both the dose and the pulse energy are key parameters in the formation of nanogratings including their pseudo-periodicity. Finally, inside the plasma dense region, the formation of porous nanolayers is observed in silica, and silica-rich glasses [14]. The nanopores constituting these

nanolayers typically show a size of few tens of nm. In 2013 the presence of free molecular $O_2$ was detected inside these nanopores [15]. In the same work, the birth of these nanopores was associated to a tensile stress-assisted nanocavitation and a "soft" Coulomb force necessary to overcome the oxygen binding energy and to form nanopores by recombination (to form $O_2$) upon an intense stress field. A cavitation mechanism was also proposed in the formation of these nanopores, building on the theory developed by Grady on spall fracture of matter [16]–[18].

A direct observation from the above introductory discussion is that the electron plasma is self-organized in hot (dense) nanoplanes, and this is *a priori* not composition limited, as it is the case for surface nanogratings (LIPSS, Laser-induced periodic surface structures) [19]. While the origin(s) of nanogratings formation has not been fully elucidated yet, these features have been observed in a variety of glasses, and most specifically oxides and silica-based glasses. These include but are not limited to silica [1], [9], [20], germanosilicates [21], [22], sodium silicates [23], germania [20], [24], sodium germanates [25], alkali-free aluminoborosilicate (AF32 Schott) [26], alkali-containing borosilicate (BK7 Schott, Borofloat 33 Schott), and titanium silicate (ULE Corning) [20], [27]. However, it is worth pointing out that for some glasses such as $SiO_2$, $GeO_2$, or Borofloat 33, the laser-processing window to form nanogratings is large. On the opposite, glasses such as AF32 or likely BK7 have shown a narrower window. For BK7, only a weak birefringence response was shown, without laser-polarization dependence of the slow/fast axis orientation nor supported by electron microscope techniques demonstrating the presence of organized porous nanogratings.

In this context, this work provides insights on the relative difficulty to form nanogratings in some of these commercial glasses. The goal is to describe, based on a viscosity approach, the ability for a glass to yield permanent formation of nanogratings. First, five commercial glasses are selected, namely BK7, AF32, Borofloat 33, $GeO_2$, and $SiO_2$ (SuprasilCG). In addition of $SiO_2$ being the backbone material of many of today's photonic applications, all these glasses present interests for diverse applications. This includes, among others, mid-infrared optical devices ($GeO_2$), silicon wafer assembly in semi-conductor industry and flat glass for display (AF32), precision optics for space telescope substrates, or photovoltaic, medical technologies (Borofloat 33), visible and near-infrared micro-optic elements, prisms (BK7). The selected glasses are then irradiated by a fs-laser and using similar conditions. This systematic work allows a direct comparison between the glass samples and their respective nanogratings processing windows. The observed differences are then tentatively linked to viscosity-driven mechanisms, framing the existence of the aforementioned nanogratings processing window. Consequently, this work is expected to establish guidelines for future glass development when nanogratings 3D structuring is required for a wide range of applications.

## II. Experimental details

To investigate the effect of glass composition, hence viscosity, on the ability to form nanogratings, a series of five bulk glasses was selected based on literature results and viscosity profile (more information on this later in the paper): BK7, AF32, Borofloat 33, $GeO_2$, and $SiO_2$ (SuprasilCG). Each glass sample, taking the form of a plate was irradiated in similar conditions using a femtosecond laser (Satsuma, Amplitude Système, Bordeaux, France) having a central wavelength at 1030 nm and a numerical aperture objective NA = 0.6, at a pulse duration $\tau_p$ of 800 fs. In cartesian coordinates, z is the laser beam direction, and the laser scanning irradiation is performed in the plane (x,y) perpendicular to it. This pulse duration was chosen as it corresponds to a large window of nanogratings formation in $SiO_2$, AF32, and Borofloat 33 [26]. In this work, the investigation of nanogratings existence was probed in a pulse energy ($E_p$, in µJ) – repetition rate (RR, in kHz) landscape. There exists a variety of possible laser-induced transformations in oxide glasses, such as formation of defects, densification, nanogratings and/or void formation, elemental migration, partial crystallization, and appearance of a stress field [28]–[30]. Therefore, an experimental procedure must be employed to decipher if there is, or not, the presence of nanogratings inside the laser track. First, each glass sample is irradiated using two different laser writing configurations: laser writing polarization parallel (along y) and perpendicular (along x) to the scanning direction (along y). Consequently, polarized optical microscopy (Olympus BX51) is used to quantify the birefringence response, along with its sensitivity (neutral axis orientation, amplitude) with respect to light polarization orientation, characteristic of nanogratings. Additionally, a complementary electron microscopy analysis (FEG–SEM Zeiss Supra 55 VP) was performed on the laser tracks (x,z plane) to ensure the existence of porous nanolayers and nanopores, therefore confirming the polarized optical microscopy results.

The data taken for all commercial glasses investigated where provided by the glass suppliers (technical datasheets). Additionally, the glass viscosities temperature dependence ($\eta(T)$) were fitted using the Vogel–Fulcher–Tammann (VTF) equation. The viscosity data for $GeO_2$ where taken from [31], [32] while other

parameters where taken from [33], [34]. It is worth mentioning at this point that most of the viscosity data points, in log($\eta$, in Pa·s), are comprised between 3 and 13. Therefore beyond these values the confidence interval would be drastically reduced.

## III. Results and discussion

*III.1. Domain of nanogratings existence*

The formation of nanogratings in the $E_p$-RR landscape was investigated for $SiO_2$ (Suprasil), $GeO_2$, Borofloat 33, AF32, and BK7 glasses. The domain of nanogratings existence for each glass is shown in Fig. 1(a). As can be observed, the glass material strongly influences the ability to imprint nanogratings from the "self-organized" plasma. For BK7, which presents the smallest nanogratings window, porous nanogratings could be observed nevertheless, as shown in Fig. 1(b), but for very specific conditions (<100 kHz, and for typ. 50,000 pulses/µm). Additionally, and for all glasses, an example of measured retardance values (i.e., birefringence x nanogratings length along z axis) with respect to energy and at a constant RR = 50 kHz is provided in Fig. 1(c). Each measured retardance data point retardance has a ± 5 nm uncertainty. The nanogratings window is the largest for $SiO_2$, intermediate for $GeO_2$, Borofloat 33, and AF32, and is extremely reduced for BK7 (an alkali "rich" borosilicate). Correspondingly, much higher values of retardance are found in silica glass compared to AF32 and BK7, which agree with the tendency to form nanogratings more easily in $SiO_2$ or $GeO_2$ that are strong network formers.

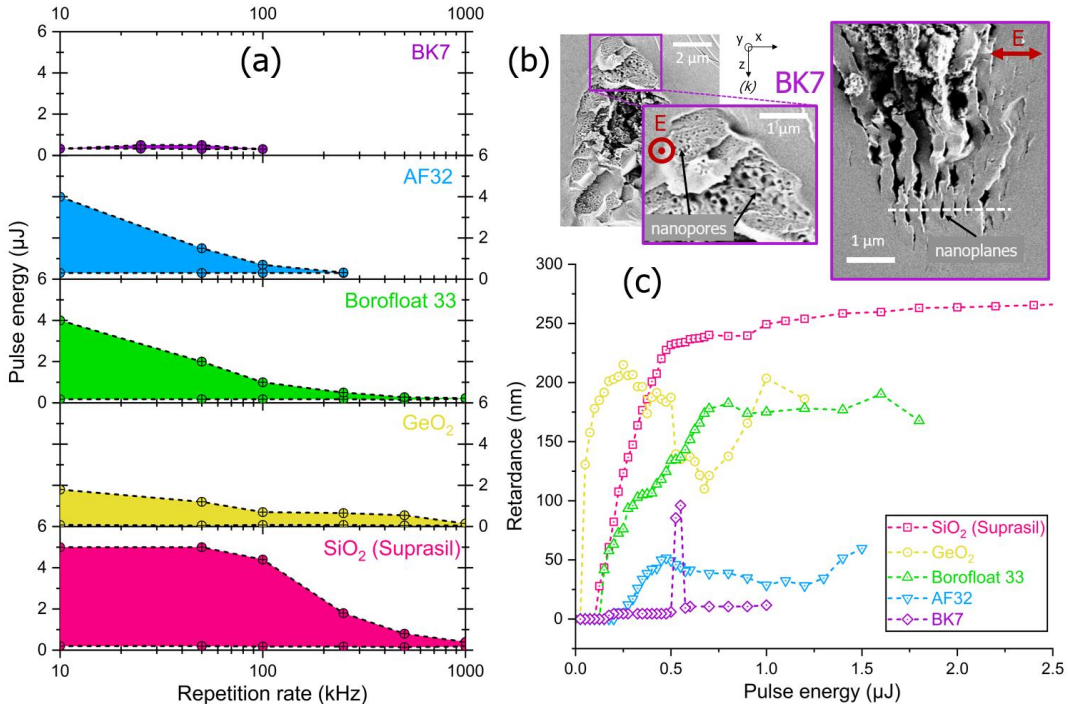


**Fig. 1.** a) Determination of observed nanogratings in an energy-repetition rate landscape for five glasses: $SiO_2$ (Suprasil), $GeO_2$, Borofloat 33, AF32, and BK7. b) Illustration of nanogratings observed in BK7 from scanning electron microscopy analysis; conditions are pulse duration = 800 fs, writing speed = 1 µm/s, RR = 25 kHz, $E_p$ = 0.6 µJ, focal depth = 300 µm. c) Evolution of retardance as a function of pulse energy (800 fs, 50 kHz, NA = 0.6); each data point has a ± 5 nm uncertainty.

The principal aim of this paper is to highlight the link between nanogratings window and glass viscosity behavior with temperature. Therefore, and to better appreciate the discussion in the next Section, below is briefly discussed how the temperature elevation upon fs-laser irradiation is impacted in an $E_p$-RR landscape. There exist two principal situations when considering the $E_p$ – RR landscape as in Fig. 1(a):

*i) Low RR, increasing $E_p$.* From the heat equation (Fourier's law), the temperature profile distribution in space is unchanged, but the deposited heat inside the material would increase. Consequently, the maximal temperature increase ($\Delta T$) at the pulse center would also increase, following a general form of $\Delta T \sim aE_p/\rho C_p V$. Here $a$ is the fraction of the pulse energy absorbed by the material and effectively transmitted to the glass phonons, $\rho$ and $C_p$, respectively, are the glass density and heat capacity, and $V$ the volume within which the pulse energy is absorbed. It is worth pointing out that $a$ is a function of fluence (e.g., in silica glass [35]), and such temperature

rise has already been investigated for several glass matrices including silica or Borofloat 33 [36], [37]. As $E_p$ is increased (and so $\Delta T$), the spatial volume for which the temperature is beyond a transformation temperature threshold (e.g., formation of nanogratings) would be enlarged.

*ii) High RR, fixed $E_p$.* This condition is also called "heat accumulation regime". In this regime, the heat generated by a pulse in the irradiated area does not have enough time to fully diffuse away before the next pulse is delivered. The characteristic time to evacuate the heat can be estimated as $\tau_{th} \approx \omega_0^2/(D_{th})$, where $D_{th} = \kappa/(\rho C_p)$ is the diffusion coefficient, $\kappa$ is the thermal conductivity, and $\omega_0$ is the characteristic length corresponding to the beam waist radius (typ. 1.5 µm). As an example, this gives $D_{th}$ ($SiO_2$) ≈ $8.9\times10^{-7}$ m²/s and $D_{th}$ (BK7) ≈ $5.2\times10^{-7}$ m²/s, and consequently $\tau_{th}$ ($SiO_2$) ≈ 2.5 µs while $\tau_{th}$ (BK7) ≈ 4.3 µs. Turning these values into heat accumulation threshold frequencies, this gives $f_{th}$ ($SiO_2$) ≈ 400 kHz and $f_{th}$ (BK7) ≈ 230 kHz. Consequently, one would expect heat accumulation to be more pronounced in BK7 with respect to $SiO_2$.

From this short discussion and circling back to Fig. 1(a), one can note that the narrowing of the nanogratings window typically comes from both lower $E_p$ and RR values. Consequently, the "temperature sensitivity" or "temperature interval" to make nanogratings appears reduced in glasses such as BK7 with respect to $SiO_2$. This reasoning is the starting point of the next Section dedicated to establishing a rational approach.

### *III.2. Rationale for a viscosity-based approach*

Both the mechanisms of cavitation and erasure of the nanogratings take their roots in the material ability to break and reform itself in a time-temperature frame. In the following Section, the upper and lower limits of nanogratings existence are discussed on a temperature dependent viscosity basis.

#### *Minimum viscosity to induce cavitation*

When ultrashort laser pulses are deposited inside a large bandgap oxide glass as in our case, the pulse energy is absorbed by the glass material mostly through nonlinear effects (multi-photon absorption and tunnel ionization) and a significant part is subsequently transformed into heat through electron-lattice energy transfer. This takes a maximum of few 10s of picoseconds in most glasses [4], [38] while the maximum thermodynamic temperature increases as already discussed in the previous Section, reaching typically values of few thousands of degrees [36], [37]. The generated heat cannot escape the irradiated volume in the time of a pulse duration (typ. 100-1000 fs). This is the condition of so called "thermal confinement". For such condition to be valid, the pulse duration $\tau_p$ must be shorter than the thermal relaxation time $\tau_{th}$ [39]. As calculated above, for silica $\tau_{th} \approx 2.5$ µs and therefore $\tau_p << \tau_{th}$ for fs or ps laser pulses. The criterion of thermal confinement is thus satisfied. Additionally, if there are no significant strain or volume changes of the medium during heating, we are in the condition of so-called "stress confinement" [39]. For this second condition to be valid, the required time for the pulse to heat the sample must be shorter than the characteristic acoustic relaxation time $\tau_{ac} \approx 2\omega_0/c_s$, with $c_s$ being the sound speed (≈ 6000 m/s for silica glass). This gives $\tau_{ac} \approx 500$ ps whereas the electron-phonon coupling time is on the order of 10 ps for silica and therefore the criterion of stress confinement is also satisfied. Therefore, the experimental conditions are met to yield nanocavitation in the glass samples.

Subsequently to this and following the wave equation from isotropic solids, the maximum tensile stress internally developed (a kind of negative pressure) can be approximated as $p \approx B\beta\Delta T$. Here $B$ is the bulk modulus (36 GPa for silica), $\beta$ is the volumetric expansion coefficient ($\beta \approx 3\alpha \approx 3\times5.5\times10^{-7}$ $K^{-1}$ for silica), and $\Delta T$ is the temperature elevation following the pulse energy deposition. Some caveats are worth pointing out: we use solid properties for each material (bulk modulus, thermal expansion coefficient), and assume them constant with respect to temperature. Although this is questionable, it provides a guideline for reasoning. Interestingly, it must be pointed out that the resulting tensile stress is drastically different depending on the glass material considered. For a moderate temperature increase (e.g., 1000 °C [37]), there is an order of magnitude difference between silica (≈ 60 MPa) and BK7 (≈ 1160 MPa). Once the tensile stress is developed, a positive pressure difference exists between the initiated pore and the surrounding material. Beyond a certain critical tension, the heated glass volume is expected to experience cavitation [16], [17]. For silica glass, Rudenko *et al.* demonstrated that the minimal temperature for cavitation is set when the viscosity is on the order of $10^6$ Pa·s [17], [18]. Such temperature is very close to the softening point ($T_{soft}$) of the material, i.e., $10^{7.6}$ P or $10^{6.6}$ Pa·s, 1873 K for Suprasil. This temperature of cavitation is calculated for a viscosity of $\eta_{cav} \approx B\xi\tau_{th}^2 \approx 10^{6.3}$ Pa·s for silica, using a strain rate of $\xi = 10^7 s^{-1}$, so indeed close to the softening temperature as previously stated. In this work we use $\xi \approx p/(B \times \tau_{ac})$ which falls within the magnitude of $\eta_{cav}$ values provided by Rudenko *et al.* [17], [18]. Written only in terms of glass and laser

parameters, this gives $\eta_{cav} \approx p \times \left(\frac{\tau_{th}^2}{\tau_{ac}}\right) = \frac{\omega_0^3 \cdot p \cdot c_S}{2 \cdot D_{th}^2} = \frac{\omega_0^3 \cdot 3\alpha \cdot B \cdot \Delta T \cdot c_S \cdot \rho^2 \cdot C_p^2}{2\kappa^2}$. Some key properties, from the above discussion, are provided in Table 1. It is worth mentioning that for a constant $p$ value (e.g., 100 MPa), $\eta_{cav}$ is comprised between $10^{6.1}$ and $10^{6.6}$ Pa·s for all glasses considered. The cavitation temperature ($T_{cav}$) in Table 1 deduced from the VTF fit performed for each glass is found close to $T_{soft}$.

**Table 1** Typical values including cavitation and erasure criteria and temperatures for the glasses investigated.

| Glass material | $p \approx B \cdot \beta \cdot \Delta T$[1] (MPa) | $\eta_{cav} \approx p \cdot (\tau_{th}^2/\tau_{ac})$ (Pa·s) | $T_{cav}$ ($T_{soft}$) (°C) | $\eta_{max} \approx p \cdot \tau_{th}$ | $T_{max}$ (°C) | $T_{max}$ - $T_{cav}$ (°C) |
|---|---|---|---|---|---|---|
| $SiO_2$ (Suprasil) | 60 | $10^{5.9}$ | 1688 (1600) | $10^{2.2}$ | 2298 | 610 |
| $GeO_2$ | 440 | $10^{7.1}$ | 838 (894) | $10^{3.3}$ | 1332 | 494 |
| Borofloat 33 | 350 | $10^{6.9}$ | 797 (821) | $10^{3.1}$ | 1254 | 457 |
| AF32 | 550 | $10^{7.1}$ | 937 (969) | $10^{3.2}$ | 1277 | 340 |
| BK7 | 1160 | $10^{7.6}$ | 675 (720) | $10^{3.7}$ | 906 | 231 |

[1]: Given for a $\Delta T$ value of 1000 °C, and $p$ is a tensile (negative) pressure.

*Maximum viscosity before growth instability or erasure of nanogratings*

Following the formation of nanopores beyond the cavitation temperature, the stability of a cavitated pore, i.e., its ability to exist, must be considered. From this view, one must investigate what are the key mechanisms that drive the pore size evolution (either its growth or collapse) once it is formed. This can be achieved through the analysis of the non-dimensional Rayleigh-Plesset (R-P) equation, which takes the following form [40]:

$$(\bar{R})\ddot{\bar{R}} + \frac{3}{2}\left(\dot{\bar{R}}\right)^2 = -\left(\frac{\tau}{\tau_p}\right)^2 \frac{p_\infty(t) - p_v}{p_{\infty\,ref} - p_v} - \left(\frac{\tau}{\tau_s}\right)^2 \frac{1}{\bar{R}} - \frac{\tau}{\tau_v}\frac{\dot{\bar{R}}}{\bar{R}} \qquad (1),$$

where $\bar{R} = R/a$ is a dimensionless radius near unity ($a$ is a characteristic length, typ. the initial pore radius in few or tens of nm), $\tau$ is the characteristic time of bubble evolution, $p_{\infty\,ref}$ is the reference pressure taken far away from the pore, $p_v$ the pressure inside the pore ($p_{\infty\,ref} - p_v = p$ as defined above), and $\dot{\bar{R}}$ and $\ddot{\bar{R}}$ are the first and second derivatives of the radius with respect to time. In the above equation three characteristic times are set: a pressure one $\left(\tau_p = a\sqrt{\frac{\rho}{p}}\right)$, a surface tension one $\left(\tau_s = a\sqrt{\frac{\rho a}{2\sigma}}\right)$ with $\sigma$ being the surface tension, and a viscosity one $\left(\tau_v = \frac{\rho a^2}{4\eta}\right)$ [40]. These characteristic times can be plotted as a function of the pore radius, as shown in Fig. 2.

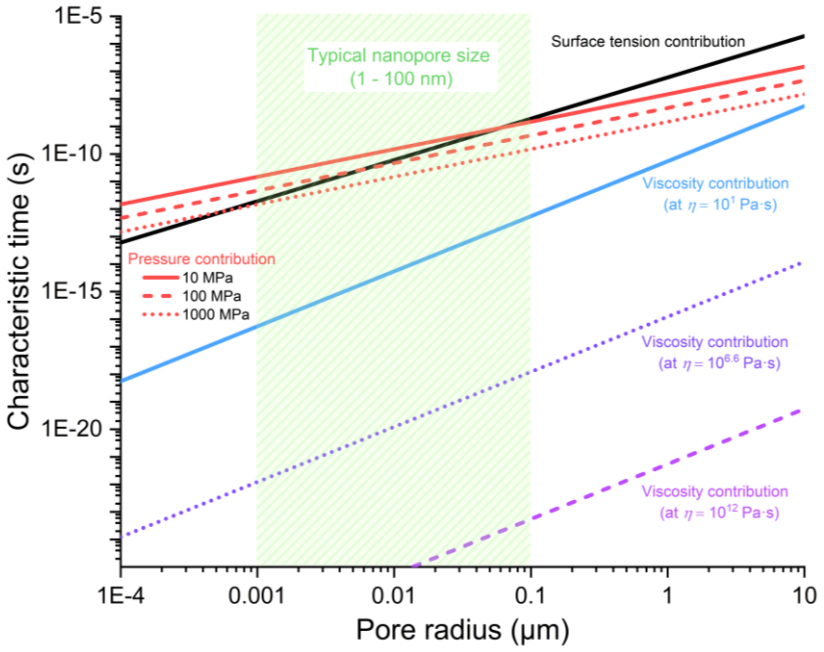


**Fig. 2.** Evolution for characteristic time as a function of pore radius using the non-dimensional Rayleigh-Plesset equation. The impact of pressure (set at $\Delta p$ = 10, 100, 1000 MPa), surface tension (with $\sigma$ = 0.3 J·m$^{-2}$), and viscosity can be estimated (the contribution with the smallest characteristic time dominates).

The contribution holding the lowest characteristic time is the dominant factor in the evolution of the nanopores. Typical values for silica at the softening point ($10^{6.6}$ Pa·s) for a 5 nm pore radius would give $\tau_v \approx 10^{-21}$ s, $\tau_s$ and $\tau_p \approx 10^{-11}$ s. At the melting temperature (defined as $10^{1}$ Pa·s) $\tau_v \approx 10^{-15}$ s, which is still 4 orders of magnitude lower than $\tau_p$. It is indicative that the dynamics of bubble evolution (growth/collapse) is almost exclusively driven by glass viscosity.

Consequently, a criterion must be selected as an indication of pore instability. The use of the dimensionless Peclet number ($Pe$) was proposed to set the limit of "unstable" hydrodynamic growth of the nanopores [41]. The limit is set for $Pe = \frac{p \times \tau_{th}}{\eta_{max}} = 1$, giving the criterion $\eta_{max} \sim p \times \tau_{th}$. For silica glass it gives a value of ~$10^{2.2}$ Pa·s, corresponding to a $T$ ~ 2300 °C. The calculated $\eta_{max}$ for the glasses considered in this study are reported in Table 1. The $\eta_{max}$ value corresponds to the maximal viscosity beyond which a viscous growth would prevent stable nanopores to exist. All the glasses fall within a $\eta_{max}$ interval of $10^{2.2}$ - $10^{3.7}$ Pa·s. Finally, it is worth pointing out that the stress induced upon heating will ultimately relax, yielding to a drop in the initial tensile pressure $p$. From this perspective and the above equation, one can notice that $\eta_{max}$ would be lower. Therefore, a potential collapse of the pore is anticipated if the pressure contribution becomes less important than that of the surface tension term [40], [42]. This competing effect is exemplified in Fig. 2, where low pressures such as 10 MPa would tend to promote collapse ($\tau_p > \tau_s$), while higher pressures such as 1000 MPa would yield to growth ($\tau_p < \tau_s$). In an intermediate regime, the pore could experience either growth or collapse, and perhaps both within the laser track location. This suggests that there may be a competing effect between pore growth and collapse depending on the temperature/viscosity and conditions considered. However, beyond $\eta_{max}$ the existence of nanopores is expected to be compromised and this viscosity value is kept as the upper bound of nanogratings existence.

*III.3. Prediction of nanogratings imprinting in various glass systems*

From the above discussion, it becomes clear that the temperature difference between the $T_{max}$ and $T_{cav}$, reported in Table 1, must be maximized for a glass in order to present a larger nanogratings window. In Fig. 3(a) the viscosity as a function of temperature for multiple oxide glasses (in addition to the ones discussed in this paper) is reported. An estimated domain of nanogratings existence is provided in Fig. 3(b), by taking the temperature difference between $T_{max}$ (set as $\eta = 10^{3.0}$ Pa·s) and $T_{soft}$ ($\eta = 10^{6.6}$ Pa·s), respectively upper and lower bounds.

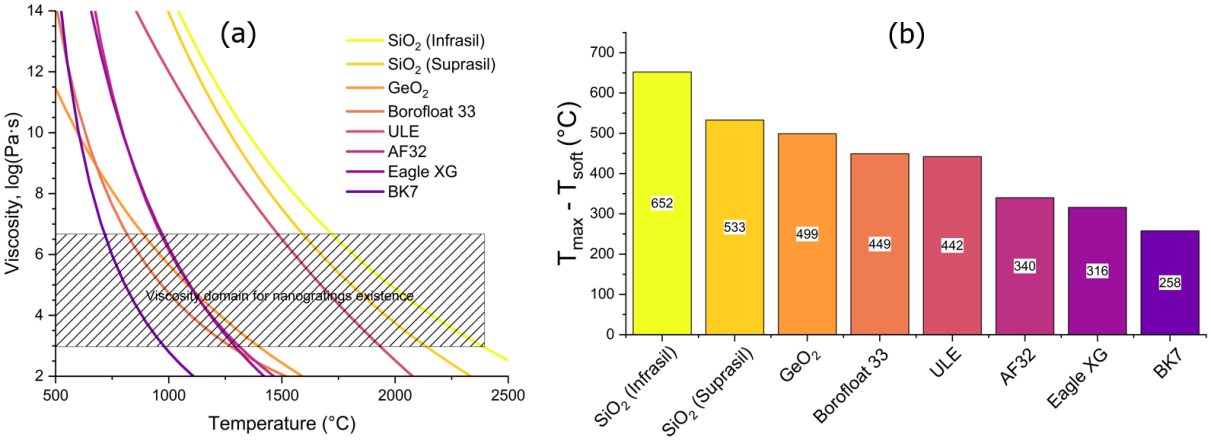


**Fig. 3.** a) Viscosity as a function of temperature for a variety of commercial and typical glasses, along with an estimated domain of nanogratings existence from $T_{soft}$ ($\eta = 10^{6.6}$ Pa·s) to $T_{max}$ ($\eta = 10^{3.0}$ Pa·s). b) Temperature difference ($T_{max} - T_{soft}$) as a function of glass composition. A larger value suggests a wider processing window (with respect to temperature) to form nanogratings.

The predicted "effectiveness" to imprint "stable" nanogratings in the selected glasses, in a sense that they can be observed after laser irradiation, agrees with the results reported in Fig. 1, where BK7 presents the lowest temperature interval and the narrowest nanogratings window, while it is the opposite for silica. Moreover, these findings concur with literature data. For example, in Ref. [26], for 800 fs pulse duration, the nanogratings window was found larger for $SiO_2$, the Borofloat 33, and finally AF32, which is what is found and predicted herein (Figs. 1a and 3b). In $GeO_2$ and $GeO_2$-doped $SiO_2$ glasses, it was found relatively easy to induce nanogratings with various sets of laser parameters and writing conditions [20]–[22], [24], [25]. Moreover, the birefringence response observed in Ref. [27] for BK7 was likely due to nanogratings. Indeed, from this work we demonstrated the SEM

observation of nanogratings in BK7 (Fig. 1b), while both the experimentally and predicted narrow nanogratings window agrees with the difficulty in this cited work to detect the nanopores/nanoplanes using scanning electron microscopy (SEM).

Several other aspects are worth discussing. First, BK7 displays a much lower bandgap energy compared to silica (~3.5 eV versus ~9 eV). Consequently, even with a 3-photon nonlinear absorption (in our case $\lambda$ = 1030 nm, i.e., 1.2 eV), the formation of bulk nanogratings is still possible. Secondly, in some glasses such as alkali-rich glasses (e.g., $Na_2O$-$SiO_2$ [23]) a large number of pulses is required to trigger nanogratings. Interestingly, network modifiers are found to migrate outward of the irradiated volume [30]. A direct consequence, based on our work, could be a local variation in the glass viscosity enabling not only the formation of nanogratings at short time scale but also their survival to the heating-cooling processes during pulse deposition.

Finally, several studies have highlighted, based on thermo-mechanical arguments, strong evidences of a void-to-nanogratings transitioning upon progressive laser irradiation (e.g., Refs. [43], [44]). Although this requires a more in-depth analysis based on the proposed approach, several aspects are anticipated herein. High tensile strength, generated induced by high energy deposition, would favor void formation as the pressure contribution would overcome the surface energy term (Fig.3), yielding viscous growth of the nanopores. Additionally, the description of higher thermal gradients, associated with the fastest growth of nanobubbles in the laser track head as described in Ref. [44] is in agreement with our findings. While the topic of another study, this approach could also frame the existence domain of void-like transformations.

## IV. Conclusion

Understanding the formation of nanogratings inside silicate and germanate glasses is an attractive research field, since these sub-wavelength and self-organized structures enable miniaturized functionalization and unique properties. In this context, this work addresses the challenges to imprint, or not, nanogratings, through a viscosity approach. It is shown, building from previous work, that the nanogratings domain is bound between two limits: i) a low temperature one, corresponding to a cavitation mechanism, and for which the viscosity is situated at ~$10^{6.6}$ Pa·s, and ii) a high temperature one when the pores experience either growth or collapse, this time for a viscosity value typically around ~$10^{3.0}$ Pa·s. These predictions are validated by experimental work performed on five glasses, for which nanogratings domains are either large ($SiO_2$), intermediate ($GeO_2$, AF32, Borofloat 33), and narrow (BK7). The results agree with the literature and the proposed viscosity approach. A direct consequence of this work is to demonstrate that nanogratings can be achieved in most, if not any, glasses. However, the processing windows can be drastically different, and a systematic analysis must be undertaken to find the adequate conditions for which nanogratings can survive the laser-irradiation process.

Future work includes simulation of the temperature elevation during the irradiation process for each glass composition. This will help to target and anticipate in which conditions the temperature range, hence viscosity range (see Fig. 3) corresponding to the formation of nanogratings, can be achieved.


## Funding

This research was funded by Agence Nationale pour la Recherche, FLAG-IR project, grant number ANR-18-CE08-0004-01 and CNRS Défi Instrumentation aux Limites, UltraBragg project. Qiong Xie acknowledges the China Scholarship Council (CSC) for the funding her PhD fellowship.


## References


[1] Y. Shimotsuma, P. G. Kazansky, J. Qiu, and K. Hirao, "Self-Organized Nanogratings in Glass Irradiated by Ultrashort Light Pulses," *Phys. Rev. Lett.*, vol. 91, no. 24, pp. 247405(1)-247405(4), Dec. 2003, doi: 10.1103/PhysRevLett.91.247405.

[2] J. Tian *et al.*, "Spectral dependence of femtosecond laser induced circular optical properties in silica," *OSA Contin.*, vol. 2, no. 4, pp. 1233–1242, 2019, doi: 10.1364/osac.2.001233.

[3] J. Tian, M. Lancry, B. Poumellec, E. Garcia-Caurel, and R. Ossikovski, "Study of femtosecond laser induced circular optical properties by Mueller matrix spectropolarimetry," *Opt. Lett.*, vol. 42, no. 20, pp. 4103–4106, 2017, doi: 10.1364/ol.42.004103.

[4] E. Mazur and R. Gattass, "Femtosecond laser micromachining in transparent materials," *Nat. Photonics*, vol. 2, no. 4, pp. 219–225, 2008, doi: 10.1038/nphoton.2008.48.

[5] S. J. Mihailov *et al.*, "Extreme Environment Sensing Using Femtosecond Laser-Inscribed Fiber Bragg Gratings," *Sensors*, vol. 17, no. 12, 2017, doi: 10.3390/s17122909.

[6] B. Zhang, X. Liu, and J. Qiu, “Single femtosecond laser beam induced nanogratings in transparent media - Mechanisms and applications,” *J. Mater.*, vol. 5, pp. 1–14, 2019, doi: .1037//0033-2909.I26.1.78.
[7] Y. Shimotsuma *et al.*, “Ultrafast manipulation of self-assembled form birefringence in glass,” *Adv. Mater.*, vol. 22, no. 36, pp. 4039–4043, 2010, doi: 10.1002/adma.201000921.
[8] M. Beresna, M. Gecevičius, and P. G. Kazansky, “Polarization sensitive elements fabricated by femtosecond laser nanostructuring of glass [Invited],” *Opt. Mater. Express*, vol. 1, no. 4, pp. 783–795, 2011, doi: 10.1364/ome.1.000783.
[9] R. Stoian, “Volume photoinscription of glasses: three-dimensional micro- and nanostructuring with ultrashort laser pulses,” *Appl. Phys. A Mater. Sci. Process.*, vol. 126, no. 6, pp. 1–30, 2020, doi: 10.1007/s00339-020-03516-3.
[10] R. Taylor, C. Hnatovsky, and E. Simova, “Applications of femtosecond laser induced self-organized planar nanocracks inside fused silica glass,” *Laser Photonics Rev.*, vol. 2, no. 1–2, pp. 26–46, 2008, doi: 10.1002/lpor.200710031.
[11] M. Beresna, M. Gecevičius, P. G. Kazansky, T. Taylor, and A. V. Kavokin, “Exciton mediated self-organization in glass driven by ultrashort light pulses,” *Appl. Phys. Lett.*, vol. 101, no. 5, pp. 053120(1)-053120(4), 2012, doi: 10.1063/1.4742899.
[12] R. Buschlinger, S. Nolte, and U. Peschel, “Self-organized pattern formation in laser-induced multiphoton ionization,” *Phys. Rev. B - Condens. Matter Mater. Phys.*, vol. 89, no. 18, pp. 1–10, 2014, doi: 10.1103/PhysRevB.89.184306.
[13] A. Rudenko, J. P. Colombier, and T. E. Itina, “From random inhomogeneities to periodic nanostructures induced in bulk silica by ultrashort laser,” *Phys. Rev. B*, vol. 93, no. 7, pp. 075427(1)-075427(13), 2016, doi: 10.1103/PhysRevB.93.075427.
[14] J. Canning, M. Lancry, K. Cook, A. Weickman, F. Brisset, and B. Poumellec, “Anatomy of a femtosecond laser processed silica waveguide,” *Opt. Mater. Express*, vol. 1, no. 5, pp. 998–1008, 2011, doi: 10.1364/ome.1.000998.
[15] M. Lancry, B. Poumellec, J. Canning, K. Cook, J.-C. Poulin, and F. Brisset, “Ultrafast nanoporous silica formation driven by femtosecond laser irradiation,” *Laser Photonics Rev.*, vol. 7, no. 6, pp. 953–962, 2013, doi: 10.1002/lpor.201300043.
[16] D. E. Grady, “the spall strength of condensed matter,” *J. Mech. Phys. Solids*, vol. 36, no. 3, pp. 353–384, 1988.
[17] A. Rudenko, J. P. Colombier, and T. E. Itina, “Nanopore-mediated ultrashort laser-induced formation and erasure of volume nanogratings in glass,” *Phys. Chem. Chem. Phys.*, vol. 20, no. 8, pp. 5887–5899, 2018, doi: 10.1039/c7cp07603g.
[18] A. Rudenko, “Numerical study of ultrashort laser-induced periodic nanostructure formation in dielectric materials To cite this version : HAL Id : tel-02107355 Sciences Ingénierie et Santé Anton Rudenko Numerical study of ultrashort laser induced periodic,” 2019.
[19] M. Huang, F. Zhao, Y. Cheng, N. Xu, and Z. Xu, “Origin of laser-induced near-subwavelength ripples: Interference between surface plasmons and incident laser,” *ACS Nano*, vol. 3, no. 12, pp. 4062–4070, 2009, doi: 10.1021/nn900654v.
[20] M. Lancry *et al.*, “Nanogratings formation in multicomponent silicate glasses,” *Appl. Phys. B Lasers Opt.*, vol. 122, no. 3, pp. 1–8, 2016, doi: 10.1007/s00340-016-6337-8.
[21] F. Zimmermann *et al.*, “Femtosecond laser written nanostructures in Ge-doped glasses,” *Opt. Lett.*, vol. 41, no. 6, pp. 1161–1164, 2016, doi: 10.1364/ol.41.001161.
[22] M. Lancry, J. Canning, K. Cook, M. Heili, D. R. Neuville, and B. Poumellec, “Nanoscale femtosecond laser milling and control of nanoporosity in the normal and anomalous regimes of GeO2-SiO2 glasses,” *Opt. Mater. Express*, vol. 6, no. 2, pp. 321–330, 2016, doi: 10.1364/OME.6.000321.
[23] S. Lotarev, S. Fedotov, A. Lipatiev, M. Presnyakov, P. Kazansky, and V. Sigaev, “Light-driven nanoperiodical modulation of alkaline cation distribution inside sodium silicate glass,” *J. Non. Cryst. Solids*, vol. 479, no. October, pp. 49–54, 2018, doi: 10.1016/j.jnoncrysol.2017.10.008.
[24] F. Zhang, H. Zhang, G. Dong, and J. Qiu, “Embedded nanogratings in germanium dioxide glass induced by femtosecond laser direct writing,” *J. Opt. Soc. Am. B*, vol. 31, no. 4, p. 860, 2014, doi: 10.1364/josab.31.000860.
[25] J. Wang, X. Liu, Y. Dai, Z. Wang, and J. Qiu, “Effect of sodium oxide content on the formation of nanogratings in germanate glass by a femtosecond laser,” *Opt. Express*, vol. 26, no. 10, p. 12761, 2018, doi: 10.1364/oe.26.012761.
[26] S. S. Fedotov *et al.*, “Direct writing of birefringent elements by ultrafast laser nanostructuring in multicomponent glass,” *Appl. Phys. Lett.*, vol. 108, no. 7, 2016, doi: 10.1063/1.4941427.
[27] S. Richter *et al.*, “Laser induced nanogratings beyond fused silica - periodic nanostructures in borosilicate glasses and ULE™,” *Opt. Mater. Express*, vol. 3, no. 8, pp. 1161–1166, 2013, doi: 10.1364/OME.3.001161.

[28] S. Richter, M. Heinrich, S. Döring, A. Tünnermann, S. Nolte, and U. Peschel, "Nanogratings in fused silica: Formation, control, and applications," *J. Laser Appl.*, vol. 24, no. 4, pp. 042008(1)-042008(8), 2012, doi: 10.2351/1.4718561.
[29] Y. Wang, M. Cavillon, N. Ollier, B. Poumellec, and M. Lancry, "An Overview of the Thermal Erasure Mechanisms of Femtosecond Laser-Induced Nanogratings in Silica Glass," *Phys. Status Solidi Appl. Mater. Sci.*, vol. 218, no. 12, pp. 2100023(1)-2100023(15), 2021, doi: 10.1002/pssa.202100023.
[30] T. T. Fernandez *et al.*, "Bespoke photonic devices using ultrafast laser driven ion migration in glasses," *Prog. Mater. Sci.*, vol. 94, pp. 68–113, 2018, doi: 10.1016/j.pmatsci.2017.12.002.
[31] S. K. Sharma, D. Virgo, and I. Kushiro, "Relationship between density, viscosity and structure of GeO2 melts at low and high pressures," *J. Non. Cryst. Solids*, vol. 33, no. 2, pp. 235–248, 1979, doi: 10.1016/0022-3093(79)90052-8.
[32] E. M. Birtch, J. E. Shelby, and J. M. Whalen, "Properties of binary $GeO_2$ – $SiO_2$ glasses," vol. 47, no. 2, pp. 182–185, 2006.
[33] M. J. Weber, *Handbook of Optical Materials*, vol. 23, no. 1. CRC Press, 2003.
[34] E. M. Dianov and V. M. Mashinsky, "Germania-based core optical fibers," *J. Light. Technol.*, vol. 23, no. 11, pp. 3500–3508, 2005, doi: 10.1109/JLT.2005.855867.
[35] B. Momgaudis, V. Kudriasov, M. Vengris, and A. Melninkaitis, "Quantitative assessment of nonlinearly absorbed energy in fused silica via time-resolved digital holography," *Opt. Express*, vol. 27, no. 5, pp. 7699–7711, 2019, doi: 10.1364/oe.27.007699.
[36] M. Shimizu *et al.*, "Three-dimensional temperature distribution and modification mechanism in glass during ultrafast laser irradiation at high repetition rates," *Opt. Express*, vol. 20, no. 2, pp. 934–940, 2012, doi: 10.1364/oe.20.000934.
[37] T. Yoshino, Y. Ozeki, M. Matsumoto, and K. Itoh, "In situ micro-raman investigation of spatio-temporal evolution of heat in ultrafast laser microprocessing of glass," *Jpn. J. Appl. Phys.*, vol. 51, no. 10, 2012, doi: 10.1143/JJAP.51.102403.
[38] L. Orazi, L. Romoli, M. Schmidt, and L. Li, "Ultrafast laser manufacturing: from physics to industrial applications," *CIRP Ann. - Manuf. Technol.*, vol. 00, pp. 1–24, 2021, doi: 10.1016/j.cirp.2021.05.007.
[39] G. Paltauf and P. E. Dyer, "Photomechanical processes and effects in ablation," *Chem. Rev.*, vol. 103, no. 2, pp. 487–518, 2003, doi: 10.1021/cr010436c.
[40] J.-P. Franc, "The Rayleigh-Plesset equation: a simple and powerful tool to understand various aspects of cavitation," in *Fluid Dynamics of cavitation and cavitating turbopumps*, vol. 496, 2007, pp. 1–41.
[41] A. Rudenko *et al.*, "Spontaneous periodic ordering on the surface and in the bulk of dielectrics irradiated by ultrafast laser: A shared electromagnetic origin," *Sci. Rep.*, vol. 7, no. 1, pp. 1–14, 2017, doi: 10.1038/s41598-017-12502-4.
[42] M. S. Plesset, "The Dynamics of Cavitation Bubbles," *J. Appl. Mech.*, vol. 16, pp. 277–282, 1949, doi: 10.1080/15435075.2018.1431546.
[43] Y. Dai, A. Patel, J. Song, M. Beresna, and P. G. Kazansky, "Void-nanograting transition by ultrashort laser pulse irradiation in silica glass," *Opt. Express*, vol. 24, no. 17, p. 19344, 2016, doi: 10.1364/oe.24.019344.
[44] E. O. Kissi and Y. Bellouard, "Self-organized nanostructures forming under high-repetition rate femtosecond laser bulk-heating of fused silica," *Opt. Express*, vol. 26, no. 11, p. 14024, 2018, doi: 10.1364/oe.26.014024.